Received 12 July 2022; revised 23 July 2022; accepted 25 July 2022. Date of publication 1 August 2022; date of current version 8 August 2022.

Digital Object Identifier 10.1109/OJCOMS.2022.3195050

Low-Complexity Joint Phase Adjustment and Receive Beamforming for Directional Modulation Networks via IRS

RONGEN DONG [1], SHAOHUA JIANG [2], XINHAI HUA [3], YIN TENG [4], FENG SHU [1,4] (Member, IEEE), AND JIANGZHOU WANG [5] (Fellow, IEEE)

[1] School of Information and Communication Engineering, Hainan University, Haikou 570228, China

[2] School of Electrical and Mechanical Engineering, Weifang Vocational College, Weifang 262737, China

[3] Multimedia Video Product Department, Corporation of Zhongxing Telecommunication Equipment, Nanjing 210094, China

[4] School of Electronic and Optical Engineering, Nanjing University of Science and Technology, Nanjing 210094, China

[5] School of Engineering, University of Kent, Canterbury CT2 7NT, U.K.

CORRESPONDING AUTHOR: F. SHU (e-mail: shufeng0101@163.com)

This work was supported in part by the National Natural Science Foundation of China under Grant 62071234, Grant 62071289, and Grant 61972093; in part by the Hainan Province Science and Technology Special Fund under Grant ZDKJ2021022; in part by the Scientific Research Fund Project of Hainan University under Grant KYQD(ZR)-21008 and Grant KYQD(ZR)-21007; and in part by the National Key Research and Development Program of China under Grant 2018YFB1801102.

ABSTRACT Intelligent reflecting surface (IRS) is a revolutionary and low-cost technology for boosting the spectrum and energy efficiencies in future wireless communication network. In order to create controllable multipath transmission in the conventional line-of-sight (LOS) wireless communication environment, an IRS-aided directional modulation (DM) network is considered. In this paper, to improve the transmission security of the system and maximize the receive power sum (Max-RPS), two alternately optimizing schemes of jointly designing receive beamforming (RBF) vectors and IRS phase shift matrix (PSM) are proposed: Max-RPS using general alternating optimization (Max-RPS-GAO) algorithm and Max-RPS using zero-forcing (Max-RPS-ZF) algorithm. Simulation results show that, compared with the no-IRS-assisted scheme and no-PSM optimization scheme, the proposed IRS-assisted Max-RPS-GAO method and Max-RPS-ZF method can significantly improve the secrecy rate (SR) performance of the DM system. Moreover, compared with the Max-RPS-GAO method, the proposed Max-RPS-ZF method has a faster convergence speed and a certain lower computational complexity.

INDEX TERMS Intelligent reflecting surface, directional modulation, secrecy rate, receive beamforming, receive power sum.

I. INTRODUCTION

THE BROADCAST characteristic of wireless medium makes the transmission of information vulnerable to eavesdropping [1], [2]. As a complement to high-layer encryption techniques, physical layer security (PLS), which safeguards data confidentiality based on the information-theoretic approaches, has attracted wide attentions from academia and industry in the past decades [3]–[12]. The core principle of PLS is to exploit the characteristics of wireless channels to guarantee secure communication in the presence of eavesdroppers [13]. Directional modulation (DM), as an advanced and promising PLS communications technique, has been regarded as a useful method for fifth generation (5G) millimeter wave (mmWave) wireless communications [14], [15]. DM employs signal processing technologies like beamforming and artificial noise (AN) in radio frequency frontend or baseband, so that the signal in the desired direction can be recovered as fully as possible, while

the signal constellation diagram in the undesired direction is distorted [16]–[18].

In [19], a DM scheme using the phased arrays to generate modulation was presented, and the secure transmission was achieved since the signal was direction-dependent and purposely distorted in the undesired directions. In [20], a robust synthesis method for multi-beam DM in broadcasting systems was proposed, a robust maximum signal-to-leakage-noise ratio and maximum the signal-to-AN ratio scheme for the desired and eavesdroppers directions were presented, and an obvious bit error rate (BER) improvement over the existing orthogonal projection method along the desired direction for a given signal-to-noise ratio (SNR) was achieved. The authors in [21] developed a multi-carrier based DM framework using antenna arrays, which achieved simultaneous data transmission over multiple frequencies, and a higher data rate was achieved. In [22], the impact of imperfect angle estimation on spatial and directional modulation system was investigated, with the help of the union bound and statistics theory, the average BERs for the legitimate user and eavesdropper were derived. A scenario for DM network with a full-duplex malicious attacker was considered in [23], and three receive beamforming methods were proposed for enhancing the security performance. In [24], the authors investigated the performance of a hybrid analog and digital DM with mixed phase shifters. The closed-form expressions of signal-to-interference-plus-noise ratio, secrecy rate (SR), and BER were derived based on the law of large numbers.

The rapid development of wireless networks will lead to serious energy consumption. Different from the relay [25]–[27], intelligent reflecting surface (IRS) has been considered to be a promising green and cost-effective solution to improve the performance of wireless communication in recent years [28]–[34]. The IRS can change the phase shift of the incident electromagnetic wave, thereby intelligently reconfiguring the signal propagation environment, enhancing the power of the required received signal or suppressing interference signals [35]. A challenging scenario was considered in [36], where the eavesdropping channel was stronger than the legitimate user channel and they were highly correlated. The access point (AP) transmit beamforming and IRS reflect beamforming were jointly designed to maximize the SR. For maximizing the SR, the transmit beamforming was optimized in the IRS-aided mmWave multiple input single output system [37] and unmanned aerial vehicles transmission system [38], respectively. In [39], an IRS-aided single-cell wireless system was investigated. To minimize the total transmit power at the AP, based on semidefinite relaxation and alternating optimization methods, efficient schemes were proposed to make a tradeoff between system performance and computational complexity. The authors in [40] employed an IRS at the cell boundary to enhance the cell-edge user performance in multi-cell communication systems, in order to maximize the weighted sum rate of all users, the block coordinate descent algorithm was proposed for alternately optimizing the transmit precoding matrices at the base stations (BSs) and the passive beamforming at the IRS. In [41], an IRS-aided decode-and-forward relay network was proposed, three high-performance beamforming methods were designed to maximize the receive power. In [42], the authors investigated an IRS aided mmWave communication system using hybrid precoding at the BS. Based on the rank-one property of mmWave channels, the closed-form solution of the approximated maximum received power of user was derived.

To overcome the limitation that only one bit stream can be transmitted between the BS and user in the conventional DM networks and create controllable multipath transmission in the line-of-sight (LOS) scenario, employing IRS in DM network has been considered. An IRS-assisted DM system was proposed in [43] to utilize the multipath propagation environment for enhancing the PLS, and the closed-form expression for the SR was derived. The authors in [44] considered a double-IRS-aided two-way DM network, two transmit beamforming methods were proposed to enhance the secrecy sum rate (SSR), and an effective power allocation scheme was designed to maximize the SSR performance. In [45], in order to maximize the SR performance of IRS-assisted DM system, two alternating iterative methods, called general alternating iterative and null-space projection, were proposed. The former was of high-performance and the latter was of low-complexity.

However, the authors in [45] aimed to maximize the SR of the system by designing the transmit beamforming at the transmitter and the phase shift matrix (PSM) at the IRS, without considering the receive beamforming (RBF). In order to investigate the impact of optimizing the RBF vector and IRS PSM on the improvement of the SR performance in DM system, in this paper, we propose two alternative iterative methods to maximize the receive power sum to design the RBF and IRS PSM. The main contributions of this paper are summarized as follows:

1) To enhance the SR performance in the traditional DM networks, an IRS-aided DM network is considered. To improve the transmission security of the system and reduce the detection complexity of receiver, a general alternating optimization (GAO) of maximizing the receive power sum (Max-RPS) algorithm, called Max-RPS-GAO, is proposed firstly to attain two RBF vectors and the PSM of IRS by making use of the Rayleigh-Ritz theorem and derivative operation. The basic idea of the Max-RPS-GAO method is to jointly obtain two RBF vectors and IRS PSM by alternatively optimizing one and fixing another.
2) To receive the confidential messages (CMs) from the direct path and the IRS reflected path independently, a low-complexity Max-RPS using zero-forcing (Max-RPS-ZF) method is proposed. Here, the first RBF vector forces the signal directly from Alice to zero, and the second one forces the signal from IRS to zero. Simulation results show that, compared with the no-IRS-assisted scheme and no-PSM optimization

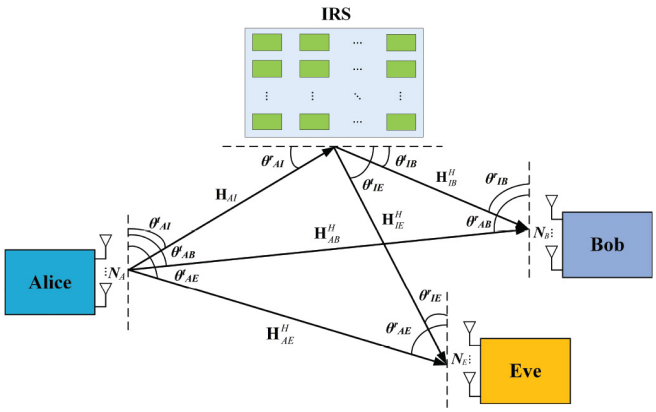

FIGURE 1. Block diagram for IRS-based directional modulation network.

scheme, the proposed IRS-assisted Max-RPS-GAO algorithm and Max-RPS-ZF algorithm can improve the SR performance of the DM system. Furthermore, compared to the proposed Max-RPS-GAO algorithm, the proposed Max-RPS-ZF algorithm converges faster with a lower computational complexity.

The remainder of this paper is organized as follows. Section II describes the IRS-based DM system model. The Max-RPS-GAO and Max-RPS-ZF methods are proposed in Section III and Section IV, respectively. Section V presents the simulation results and related analysis. Finally, we draw conclusions in Section VI.

Notations: Throughout this paper, scalar, vector, and matrix are denoted by letters of lower case, bold lower case, and bold upper case, respectively. Symbols $(\cdot)^T$, $(\cdot)^H$, $(\cdot)^{-1}$, $(\cdot)^\dagger$, and $\det\{\cdot\}$ are transpose, conjugate transpose, inverse, pseudo-inverse, and matrix determinant, respectively. The notation $\mathbf{I}_N$ denotes the $N \times N$ identity matrix. The sign $\mathbf{0}_{N\times M}$ represents the $N \times M$ matrix of all zeros.

II. SYSTEM MODEL AND PROBLEM FORMULATION

A. SYSTEM MODEL

As shown in Fig. 1, an IRS-aided DM communication network is considered in this paper, where the transmitter (Alice) is equipped with N_A antennas, IRS is equipped with M low-cost passive reflecting elements, legitimate user (Bob) and eavesdropper (Eve) are equipped with N_B and N_E antennas, respectively. In the following, it is assumed that the signals reflected more than once by the IRS are omitted due to the significant path loss [39], and the channels from Alice to IRS, Alice to Bob, Alice to Eve, IRS to Bob, and IRS to Eve are the LOS channels.

The transmit baseband signal is

$$\mathbf{s} = \sqrt{\beta_1 P_s}\mathbf{v}_1 x_1 + \sqrt{\beta_2 P_s}\mathbf{v}_2 x_2 + \sqrt{\beta_3 P_s}\mathbf{P}_{AN}\mathbf{z}, \tag{1}$$

where P_s is the total transmit power, β_1, β_2 and β_3 denote the power allocation parameters of CMs and AN, respectively, and $\beta_1+\beta_2+\beta_3 = 1$. $\mathbf{v}_1 \in \mathbb{C}^{N_A\times 1}$ and $\mathbf{v}_2 \in \mathbb{C}^{N_A\times 1}$ represent the beamforming vectors of forcing the two CMs to the desired user Bob, they satisfy $\mathbf{v}_1^H\mathbf{v}_1 = 1$ and $\mathbf{v}_2^H\mathbf{v}_2 = 1$. $\mathbf{P}_{AN}$ denotes the projection matrix for controlling the direction of AN. x_1 and x_2 are CMs which satisfy $\mathbb{E}[\|x_1\|^2] = 1$ and $\mathbb{E}[\|x_2\|^2] = 1$. $\mathbf{z}$ represents the AN vector with complex Gaussian distribution, i.e., $\mathbf{z} \sim \mathcal{CN}(\mathbf{0},\ \mathbf{I}_{N_A})$.

The received signal at Bob is given by

$$\begin{aligned} y_{Bi} &= \mathbf{u}_{Bi}^H\Big[\Big(\sqrt{g_{AIB}}\mathbf{H}_{IB}^H\mathbf{\Theta}\mathbf{H}_{AI} + \sqrt{g_{AB}}\mathbf{H}_{AB}^H\Big)\mathbf{s} + \mathbf{n}_B\Big] \\ &= \mathbf{u}_{Bi}^H\Big[\sqrt{\beta_1 P_s}\Big(\sqrt{g_{AIB}}\mathbf{H}_{IB}^H\mathbf{\Theta}\mathbf{H}_{AI} + \sqrt{g_{AB}}\mathbf{H}_{AB}^H\Big)\mathbf{v}_1 x_1 \\ &\quad + \sqrt{\beta_2 P_s}\Big(\sqrt{g_{AIB}}\mathbf{H}_{IB}^H\mathbf{\Theta}\mathbf{H}_{AI} + \sqrt{g_{AB}}\mathbf{H}_{AB}^H\Big)\mathbf{v}_2 x_2 \\ &\quad + \sqrt{\beta_3 P_s}\Big(\sqrt{g_{AIB}}\mathbf{H}_{IB}^H\mathbf{\Theta}\mathbf{H}_{AI} + \sqrt{g_{AB}}\mathbf{H}_{AB}^H\Big)\mathbf{P}_{AN}\mathbf{z} \\ &\quad + \mathbf{n}_B\Big], \quad i = 1, 2, \end{aligned} \tag{2}$$

where $\mathbf{u}_{Bi} \in \mathbb{C}^{N_B\times 1}$ represents the receive beamforming vector of Bob, $\mathbf{H}_{IB}^H = \mathbf{h}(\theta_{IB}^r)\mathbf{h}^H(\theta_{IB}^t) \in \mathbb{C}^{N_B\times M}$ represents the IRS-to-Bob channel, $\mathbf{\Theta} = \mathrm{diag}(e^{j\varphi_1}, \ldots, e^{j\varphi_m}, \ldots, e^{j\varphi_M})$ is a diagonal matrix with the phase shift φ_m incurred by the m-th reflecting element of the IRS, $\mathbf{H}_{AI} = \mathbf{h}(\theta_{AI}^r)\mathbf{h}^H(\theta_{AI}^t) \in \mathbb{C}^{M\times N_A}$ represents the Alice-to-IRS channel, $\mathbf{H}_{AB}^H = \mathbf{h}(\theta_{AB}^r)\mathbf{h}^H(\theta_{AB}^t) \in \mathbb{C}^{N_B\times N_A}$ represents the Alice-to-Bob channel, and $\mathbf{n}_B \sim \mathcal{CN}(\mathbf{0}, \sigma_B^2\mathbf{I}_{N_B})$ denotes the complex additive white Gaussian noise (AWGN) at Bob. $g_{AIB} = g_{AI}g_{IB}$ denotes the equivalent path loss coefficient of Alice-to-IRS channel and IRS-to-Bob channel, and g_{AB} is the path loss coefficient between Alice and Bob. The normalized steering vector is given by

$$\mathbf{h}(\theta) = \frac{1}{\sqrt{N}}\Big[e^{j2\pi\Psi_\theta(1)}, \ldots, e^{j2\pi\Psi_\theta(n)}, \ldots, e^{j2\pi\Psi_\theta(N)}\Big]^T, \tag{3}$$

where

$$\Psi_\theta(n) = -\frac{(n-(N+1)/2)d\cos\theta}{\lambda}, n = 1, \ldots, N, \tag{4}$$

θ is the direction angle of arrival or departure, d denotes the antenna spacing, n represents the index of antenna, and λ is the wavelength.

Similarly, the received signal at Eve is given by

$$\begin{aligned} y_{Ei} &= \mathbf{u}_{Ei}^H\Big[\Big(\sqrt{g_{AIE}}\mathbf{H}_{IE}^H\mathbf{\Theta}\mathbf{H}_{AI} + \sqrt{g_{AE}}\mathbf{H}_{AE}^H\Big)\mathbf{s} + \mathbf{n}_E\Big] \\ &= \mathbf{u}_{Ei}^H\Big[\sqrt{\beta_1 P_s}\Big(\sqrt{g_{AIE}}\mathbf{H}_{IE}^H\mathbf{\Theta}\mathbf{H}_{AI} + \sqrt{g_{AE}}\mathbf{H}_{AE}^H\Big)\mathbf{v}_1 x_1 \\ &\quad + \sqrt{\beta_2 P_s}\Big(\sqrt{g_{AIE}}\mathbf{H}_{IE}^H\mathbf{\Theta}\mathbf{H}_{AI} + \sqrt{g_{AE}}\mathbf{H}_{AE}^H\Big)\mathbf{v}_2 x_2 \\ &\quad + \sqrt{\beta_3 P_s}\Big(\sqrt{g_{AIE}}\mathbf{H}_{IE}^H\mathbf{\Theta}\mathbf{H}_{AI} + \sqrt{g_{AE}}\mathbf{H}_{AE}^H\Big)\mathbf{P}_{AN}\mathbf{z} \\ &\quad + \mathbf{n}_E\Big], \quad i = 1, 2, \end{aligned} \tag{5}$$

where $\mathbf{u}_{Ei} \in \mathbb{C}^{N_E\times 1}$ is the receive beamforming vector, $\mathbf{H}_{IE}^H = \mathbf{h}(\theta_{IE}^r)\mathbf{h}^H(\theta_{IE}^t) \in \mathbb{C}^{N_E\times M}$ denotes the IRS-to-Eve channel, $\mathbf{H}_{AE}^H = \mathbf{h}(\theta_{AE}^r)\mathbf{h}^H(\theta_{AE}^t) \in \mathbb{C}^{N_E\times N_A}$ represents the Alice-to-Eve channel, and $\mathbf{n}_E \sim \mathcal{CN}(\mathbf{0}, \sigma_E^2\mathbf{I}_{N_E})$ denotes the AWGN at Eve. $g_{AIE} = g_{AI}g_{IE}$ represents the equivalent path loss coefficient of Alice-to-IRS channel and IRS-to-Eve channel, and g_{AE} is the path loss coefficient of Alice-to-Eve channel. In what follows, we assume that $\sigma_B^2 = \sigma_E^2 = \sigma^2$ for simplicity.

Assuming that the AN is only transmitted to Eve for interference, then $\mathbf{P}_{AN}$ should satisfy

$$\mathbf{H}_{AI}\mathbf{P}_{AN} = \mathbf{0}_{M\times N_A},\ \mathbf{H}_{AB}^H\mathbf{P}_{AN} = \mathbf{0}_{N_B\times N_A}. \tag{6}$$

Let us define a large virtual CM channel as follows

$$\mathbf{H}_{CM} = \begin{bmatrix}\mathbf{H}_{AI}\\ \mathbf{H}_{AB}^H\end{bmatrix}, \tag{7}$$

then $\mathbf{P}_{AN}$ can be casted as

$$\mathbf{P}_{AN} = \mathbf{I}_{N_A} - \mathbf{H}_{CM}^H\left[\mathbf{H}_{CM}\mathbf{H}_{CM}^H\right]^{\dagger}\mathbf{H}_{CM}. \tag{8}$$

B. PROBLEM FORMULATION

Since the channels from Alice to IRS, Alice to Bob, and IRS to Bob are LOS channels, we have $\text{rank}(\mathbf{H}_{AI}) = 1$ and $\text{rank}(\mathbf{H}_{AB}) = 1$. This means that $\text{rank}(\mathbf{H}_{CM})$ is equal to or smaller than 2. There are at least $N_A - 2$ degrees of freedom for AN projection matrix $\mathbf{P}_{AN}$.

In this case, substituting (8) back into (2) and (5), we can obtain

$$\begin{aligned} y_{Bi} = \mathbf{u}_{Bi}^H\Big[&\sqrt{\beta_1 P_s}\left(\sqrt{g_{AIB}}\mathbf{H}_{IB}^H\mathbf{\Theta}\mathbf{H}_{AI} + \sqrt{g_{AB}}\mathbf{H}_{AB}^H\right)\mathbf{v}_1 x_1\\ &+ \sqrt{\beta_2 P_s}\left(\sqrt{g_{AIB}}\mathbf{H}_{IB}^H\mathbf{\Theta}\mathbf{H}_{AI} + \sqrt{g_{AB}}\mathbf{H}_{AB}^H\right)\mathbf{v}_2 x_2\\ &+ \mathbf{n}_B\Big], \quad i = 1, 2, \end{aligned} \tag{9}$$

and

$$\begin{aligned} y_{Ei} = \mathbf{u}_{Ei}^H\Big[&\sqrt{\beta_1 P_s}\left(\sqrt{g_{AIE}}\mathbf{H}_{IE}^H\mathbf{\Theta}\mathbf{H}_{AI} + \sqrt{g_{AE}}\mathbf{H}_{AE}^H\right)\mathbf{v}_1 x_1\\ &+ \sqrt{\beta_2 P_s}\left(\sqrt{g_{AIE}}\mathbf{H}_{IE}^H\mathbf{\Theta}\mathbf{H}_{AI} + \sqrt{g_{AE}}\mathbf{H}_{AE}^H\right)\mathbf{v}_2 x_2\\ &+ \sqrt{\beta_3 P_s g_{AE}}\mathbf{H}_{AE}^H\mathbf{P}_{AN}\mathbf{z} + \mathbf{n}_E\Big], \quad i = 1, 2. \end{aligned} \tag{10}$$

Let us define

$$\mathbf{H}_B = \sqrt{g_{AIB}}\mathbf{H}_{IB}^H\mathbf{\Theta}\mathbf{H}_{AI} + \sqrt{g_{AB}}\mathbf{H}_{AB}^H, \tag{11}$$

and

$$\begin{bmatrix}\sqrt{\beta_1 P_s}\mathbf{u}_{B1}^H\mathbf{H}_B\mathbf{v}_1 & \sqrt{\beta_2 P_s}\mathbf{u}_{B1}^H\mathbf{H}_B\mathbf{v}_2\\ \sqrt{\beta_1 P_s}\mathbf{u}_{B2}^H\mathbf{H}_B\mathbf{v}_1 & \sqrt{\beta_2 P_s}\mathbf{u}_{B2}^H\mathbf{H}_B\mathbf{v}_2\end{bmatrix} = \begin{bmatrix}A_b & B_b\\ C_b & D_b\end{bmatrix}. \tag{12}$$

Then, the received signal in (9) can be rewritten as

$$y_B = \begin{bmatrix}A_b & B_b\\ C_b & D_b\end{bmatrix}\begin{bmatrix}x_1\\ x_2\end{bmatrix} + \begin{bmatrix}\mathbf{u}_{B1}^H\\ \mathbf{u}_{B2}^H\end{bmatrix}\mathbf{n}_B. \tag{13}$$

The achievable rate at Bob is given by

$$\begin{aligned} R_B = \log_2\det\Bigg\{&\mathbf{I}_2 + \begin{bmatrix}A_b & B_b\\ C_b & D_b\end{bmatrix}\begin{bmatrix}A_b & B_b\\ C_b & D_b\end{bmatrix}^H\\ &\bullet\left\{\sigma^2\bullet\begin{bmatrix}\mathbf{u}_{B1}^H\\ \mathbf{u}_{B2}^H\end{bmatrix}[\mathbf{u}_{B1}\quad\mathbf{u}_{B2}]\right\}^{-1}\Bigg\}. \end{aligned} \tag{14}$$

Similarly, we define

$$\mathbf{H}_E = \sqrt{g_{AIE}}\mathbf{H}_{IE}^H\mathbf{\Theta}\mathbf{H}_{AI} + \sqrt{g_{AE}}\mathbf{H}_{AE}^H, \tag{15}$$

and

$$\begin{bmatrix}\sqrt{\beta_1 P_s}\mathbf{u}_{E1}^H\mathbf{H}_E\mathbf{v}_1 & \sqrt{\beta_2 P_s}\mathbf{u}_{E1}^H\mathbf{H}_E\mathbf{v}_2\\ \sqrt{\beta_1 P_s}\mathbf{u}_{E2}^H\mathbf{H}_E\mathbf{v}_1 & \sqrt{\beta_2 P_s}\mathbf{u}_{E2}^H\mathbf{H}_E\mathbf{v}_2\end{bmatrix} = \begin{bmatrix}A_e & B_e\\ C_e & D_e\end{bmatrix}. \tag{16}$$

Then (10) can be recasted as

$$\begin{aligned} y_E = &\begin{bmatrix}A_e & B_e\\ C_e & D_e\end{bmatrix}\begin{bmatrix}x_1\\ x_2\end{bmatrix} + \begin{bmatrix}\mathbf{u}_{E1}^H\\ \mathbf{u}_{E2}^H\end{bmatrix}\sqrt{\beta_3 P_s g_{AE}}\\ &\bullet\mathbf{H}_{AE}^H\mathbf{P}_{AN}\mathbf{z} + \begin{bmatrix}\mathbf{u}_{E1}^H\\ \mathbf{u}_{E2}^H\end{bmatrix}\mathbf{n}_E. \end{aligned} \tag{17}$$

The achievable rate at Eve is

$$\begin{aligned} R_E = \log_2\det\Bigg\{&\mathbf{I}_2 + \begin{bmatrix}A_e & B_e\\ C_e & D_e\end{bmatrix}\begin{bmatrix}A_e & B_e\\ C_e & D_e\end{bmatrix}^H\\ &\bullet\left\{\begin{bmatrix}\mathbf{u}_{E1}^H\\ \mathbf{u}_{E2}^H\end{bmatrix}\beta_3 P_s g_{AE}\mathbf{H}_{AE}^H\mathbf{P}_{AN}\mathbf{P}_{AN}^H\mathbf{H}_{AE}[\mathbf{u}_{E1}\quad\mathbf{u}_{E2}]\right.\\ &\left.+\ \sigma^2\bullet\begin{bmatrix}\mathbf{u}_{E1}^H\\ \mathbf{u}_{E2}^H\end{bmatrix}[\mathbf{u}_{E1}\quad\mathbf{u}_{E2}]\right\}^{-1}\Bigg\}. \end{aligned} \tag{18}$$

The achievable SR R_s is given by

$$R_s = \max\{0, R_B - R_E\}. \tag{19}$$

Then, the SR optimization problem is given as follows

$$\max_{\mathbf{u}_{B1},\mathbf{u}_{B2},\mathbf{\Theta}}\ R_s(\mathbf{u}_{B1}, \mathbf{u}_{B2}, \mathbf{\Theta}) \tag{20a}$$

$$\text{s.t.}\ \ \mathbf{u}_{B1}^H\mathbf{u}_{B1} = 1,\ \ \mathbf{u}_{B2}^H\mathbf{u}_{B2} = 1, \tag{20b}$$

$$|\Theta_i| = 1,\ \ i = 1, \ldots, M, \tag{20c}$$

where Θ_i is the i-th diagonal element of $\mathbf{\Theta}$, and $\arg(\Theta_i) \in [0, 2\pi)$.

For simplification of the objective function and computational convenience, we convert the SR optimization problem in (20) to the optimization problem of Max-RPS at Bob as follows

$$\max_{\mathbf{u}_{B1},\mathbf{u}_{B2},\mathbf{\Theta}}\ \beta_1 P_s\mathbf{u}_{B1}^H\mathbf{H}_B\mathbf{v}_1\mathbf{v}_1^H\mathbf{H}_B^H\mathbf{u}_{B1}$$

$$+\beta_2 P_s\mathbf{u}_{B2}^H\mathbf{H}_B\mathbf{v}_2\mathbf{v}_2^H\mathbf{H}_B^H\mathbf{u}_{B2} \tag{21a}$$

$$\text{s.t.}\ \ \mathbf{u}_{B1}^H\mathbf{u}_{B1} = 1,\ \ \mathbf{u}_{B2}^H\mathbf{u}_{B2} = 1, \tag{21b}$$

$$|\Theta_i| = 1,\ \ i = 1, \ldots, M. \tag{21c}$$

Solving this problem is a challenge since the unit modulus constraint is difficult to handle. In this case, two alternately optimizing methods are proposed to design the receive beamforming vectors and IRS PSM.

III. PROPOSED MAX-RPS-GAO SCHEME

In this section, the transmit beamforming vectors are designed firstly. Then, we will propose a GAO-based Max-RPS method to obtain the confidential message RBF vectors $\mathbf{u}_{B1}$, $\mathbf{u}_{B2}$ and IRS PSM $\mathbf{\Theta}$ by alternately optimizing one and fixing another.

A. DESIGN OF THE TRANSMIT BEAMFORMING VECTORS

Firstly, to fix CM precoding vectors $\mathbf{v}_1$ and $\mathbf{v}_2$, channel matrix $\mathbf{H}_{CM}$ in (7) is first decomposed as the singular-value decomposition (SVD)

$$\mathbf{H}_{CM} = \widetilde{\mathbf{U}}\Sigma_{CM}\widetilde{\mathbf{V}}^H = \sum_{i=1}^{2}\widetilde{\mathbf{u}}_i\widetilde{\lambda}_i\widetilde{\mathbf{v}}_i^H, \tag{22}$$

where $\widetilde{\mathbf{U}}$ and $\widetilde{\mathbf{V}}$ are unitary matrices, and Σ_{CM} is a matrix containing the singular values of $\mathbf{H}_{CM}$ and along its main diagonal. Let us define the transmit beamforming vectors $\mathbf{v}_1 = \widetilde{\mathbf{v}}_1$, $\mathbf{v}_2 = \widetilde{\mathbf{v}}_2$, where $\widetilde{\mathbf{v}}_1$ and $\widetilde{\mathbf{v}}_2$ can be obtained from the eigenvectors corresponding to the first two largest eigenvalues in Σ_{CM}, respectively.

B. OPTIMIZE RBF VECTORS $\mathbf{U}_{B1}$ AND $\mathbf{U}_{B2}$ GIVEN IRS PSM $\boldsymbol{\Theta}$

Let us define a large virtual receive channel as follows

$$\mathbf{H}_{BR} = \left[\mathbf{H}_{IB}^H \quad \mathbf{H}_{AB}^H\right]. \tag{23}$$

To obtain the initial values $\mathbf{u}_{B1}^{(0)}$ and $\mathbf{u}_{B2}^{(0)}$, the channel matrix $\mathbf{H}_{BR}$ is first decomposed as the SVD criterion

$$\mathbf{H}_{BR} = \widehat{\mathbf{U}}\Sigma_{BR}\widehat{\mathbf{V}}^H = \sum_{i=1}^{2}\widehat{\mathbf{u}}_i\widehat{\lambda}_i\widehat{\mathbf{v}}_i^H, \tag{24}$$

where $\widehat{\mathbf{U}}$ and $\widehat{\mathbf{V}}$ are unitary matrices, and Σ_{BR} represents a matrix containing the singular values of $\mathbf{H}_{BR}$ and along its main diagonal. We define the RBF $\mathbf{u}_{Bi}^{(0)} = \widehat{\mathbf{u}}_i$, where $\widehat{\mathbf{u}}_i$ can be derived from the eigenvectors corresponding to the first two largest eigenvalues in Σ_{BR}.

To simplify the expression of RPS related to the receive beamforming vectors, we regard $\boldsymbol{\Theta}$ as a given constant matrix, and the optimization problem of Max-RPS at Bob related to RBF $\mathbf{u}_{B1}$ can be simplified to

$$\max_{\mathbf{u}_{B1}} \ \beta_1 P_s \mathbf{u}_{B1}^H \mathbf{H}_B \mathbf{v}_1 \mathbf{v}_1^H \mathbf{H}_B^H \mathbf{u}_{B1} \tag{25a}$$

$$\text{s.t.} \ \ \mathbf{u}_{B1}^H \mathbf{u}_{B1} = 1. \tag{25b}$$

According to the Rayleigh-Ritz theorem in [46], the optimal $\mathbf{u}_{B1}$ can be obtained from the eigenvector corresponding to the largest eigenvalue of the matrix $\beta_1 P_s \mathbf{H}_B \mathbf{v}_1 \mathbf{v}_1^H \mathbf{H}_B^H$.

Similarly, given the determined or known $\mathbf{u}_{B1}$ and $\boldsymbol{\Theta}$, the subproblem to optimize $\mathbf{u}_{B2}$ can be expressed as follows

$$\max_{\mathbf{u}_{B2}} \ \beta_2 P_s \mathbf{u}_{B2}^H \mathbf{H}_B \mathbf{v}_2 \mathbf{v}_2^H \mathbf{H}_B^H \mathbf{u}_{B2} \tag{26a}$$

$$\text{s.t.} \ \ \mathbf{u}_{B2}^H \mathbf{u}_{B2} = 1. \tag{26b}$$

In accordance with the Rayleigh-Ritz theorem, the optimal $\mathbf{u}_{B2}$ can be obtained from the eigenvector corresponding to the largest eigenvalue of the matrix $\beta_2 P_s \mathbf{H}_B \mathbf{v}_2 \mathbf{v}_2^H \mathbf{H}_B^H$.

C. OPTIMIZE IRS PSM $\boldsymbol{\Theta}$ GIVEN THE RBF VECTORS $\mathbf{U}_{B1}$ AND $\mathbf{U}_{B2}$

To simplify the expression of RPS in this subsection, we regard $\mathbf{u}_{B1}$ and $\mathbf{u}_{B2}$ as the given constant vectors and define the IRS phase-shift vector $\boldsymbol{\theta}$ containing all the elements on the diagonal of $\boldsymbol{\Theta}$, i.e.,

$$\boldsymbol{\Theta} = \text{diag}\{\boldsymbol{\theta}\}, \tag{27}$$

where

$$\boldsymbol{\theta} = \left[e^{j\varphi_1}, \ldots, e^{j\varphi_i}, \ldots, e^{j\varphi_M}\right]^T. \tag{28}$$

Letting $\theta_i = e^{j\varphi_i}$ be the i-th element of $\boldsymbol{\theta}$, the IRS phase-shift vector $\boldsymbol{\theta}$ should satisfy

$$|\theta_i| = 1, \ \ \arg(\theta_i) \in [0, 2\pi), \ \ i = 1, \ldots, M. \tag{29}$$

In what follows, let us define

$$\mathbf{h}_{b1}^H = \mathbf{u}_{B1}^H \mathbf{H}_{IB}^H, \mathbf{h}_{A1} = \mathbf{H}_{AI}\mathbf{v}_1, \tag{30}$$

$$\mathbf{h}_{b2}^H = \mathbf{u}_{B2}^H \mathbf{H}_{IB}^H, \mathbf{h}_{A2} = \mathbf{H}_{AI}\mathbf{v}_2, \tag{31}$$

$$t_{h_{AIB1}}(\boldsymbol{\theta}) = \sqrt{\beta_1 P_s g_{AIB}}\mathbf{h}_{b1}^H \text{diag}\{\boldsymbol{\theta}\}\mathbf{h}_{A1} \overset{(a)}{=} \underbrace{\sqrt{\beta_1 P_s g_{AIB}}\mathbf{h}_{b1}^H \text{diag}\{\mathbf{h}_{A1}\}}_{\mathbf{w}_{h_{AIB1}}^H}\boldsymbol{\theta}, \tag{32}$$

$$t_{h_{AIB2}}(\boldsymbol{\theta}) = \sqrt{\beta_2 P_s g_{AIB}}\mathbf{h}_{b2}^H \text{diag}\{\boldsymbol{\theta}\}\mathbf{h}_{A2} \overset{(a)}{=} \underbrace{\sqrt{\beta_2 P_s g_{AIB}}\mathbf{h}_{b2}^H \text{diag}\{\mathbf{h}_{A2}\}}_{\mathbf{w}_{h_{AIB2}}^H}\boldsymbol{\theta}, \tag{33}$$

$$t_{h_{AB1}} = \sqrt{\beta_1 P_s g_{AB}}\mathbf{u}_{B1}^H \mathbf{H}_{AB}^H \mathbf{v}_1, \tag{34}$$

$$t_{h_{AB2}} = \sqrt{\beta_2 P_s g_{AB}}\mathbf{u}_{B2}^H \mathbf{H}_{AB}^H \mathbf{v}_2, \tag{35}$$

where (a) holds due to the fact that $\text{diag}\{\mathbf{a}\}\mathbf{b} = \text{diag}\{\mathbf{b}\}\mathbf{a}$. Then, the optimization problem of Max-RPS at Bob related to $\boldsymbol{\theta}$ can be expressed as follows

$$\max_{\boldsymbol{\theta}} \ \left(\mathbf{w}_{h_{AIB1}}^H\boldsymbol{\theta} + t_{h_{AB1}}\right)^H\left(\mathbf{w}_{h_{AIB1}}^H\boldsymbol{\theta} + t_{h_{AB1}}\right) + \left(\mathbf{w}_{h_{AIB2}}^H\boldsymbol{\theta} + t_{h_{AB2}}\right)^H\left(\mathbf{w}_{h_{AIB2}}^H\boldsymbol{\theta} + t_{h_{AB2}}\right) \tag{36a}$$

$$\text{s.t.} \ \ (29). \tag{36b}$$

The objective function in (36) can be rewritten as

$$f(\boldsymbol{\theta}) = \boldsymbol{\theta}^H\left(\mathbf{w}_{h_{AIB1}}\mathbf{w}_{h_{AIB1}}^H + \mathbf{w}_{h_{AIB2}}\mathbf{w}_{h_{AIB2}}^H\right)\boldsymbol{\theta} + \left(t_{h_{AB1}}\mathbf{w}_{h_{AIB1}}^H + t_{h_{AB2}}\mathbf{w}_{h_{AIB2}}^H\right)\boldsymbol{\theta} + \boldsymbol{\theta}^H \times \left(\mathbf{w}_{h_{AIB1}}t_{h_{AB1}} + \mathbf{w}_{h_{AIB2}}t_{h_{AB2}}\right) + t_{h_{AB1}}^H t_{h_{AB1}} + t_{h_{AB2}}^H t_{h_{AB2}}. \tag{37}$$

To obtain the optimal IRS phase-shift vector, we take the derivative of $f(\boldsymbol{\theta})$ with respect to $\boldsymbol{\theta}$ and set it equal to 0, i.e.,

$$\frac{\partial f(\boldsymbol{\theta})}{\partial \boldsymbol{\theta}} = \left(\mathbf{w}_{h_{AIB1}}\mathbf{w}_{h_{AIB1}}^H + \mathbf{w}_{h_{AIB2}}\mathbf{w}_{h_{AIB2}}^H\right)^T\boldsymbol{\theta}^* + \left(t_{h_{AB1}}\mathbf{w}_{h_{AIB1}}^H + t_{h_{AB2}}\mathbf{w}_{h_{AIB2}}^H\right)^T = 0, \tag{38}$$

which yields

$$\boldsymbol{\theta} = -\left(\mathbf{w}_{h_{AIB1}}\mathbf{w}_{h_{AIB1}}^H + \mathbf{w}_{h_{AIB2}}\mathbf{w}_{h_{AIB2}}^H\right)^{\dagger} \bullet \left(\mathbf{w}_{h_{AIB1}}t_{h_{AB1}}^H + \mathbf{w}_{h_{AIB2}}t_{h_{AB2}}^H\right). \tag{39}$$

D. OVERALL ALGORITHM

So far, we have completed the design of RBF vectors and PSM. The iterative idea of the proposed Max-RPS-GAO algorithm is summarized as follows: given a fixed IRS PSM $\boldsymbol{\Theta}$, the corresponding RBF vectors can be computed in a

closed-form expression iteratively; given the RBF vectors $\mathbf{u}_{B1}$ and $\mathbf{u}_{B2}$, $\boldsymbol{\theta}$ can be determined by (39) in a closed-form expression; reform $\boldsymbol{\theta} = \exp\{j\angle(\boldsymbol{\theta})\}$, $\boldsymbol{\Theta} = \text{diag}\{\boldsymbol{\theta}\}$. The alternative iteration process among $\mathbf{u}_{B1}$, $\mathbf{u}_{B2}$, and $\boldsymbol{\Theta}$ is repeated until the termination condition is met, i.e., $R_s^{(p)} - R_s^{(p-1)}$ with p being the iteration index.

The computational complexities of proposed Max-RPS-GAO algorithm is

$$\mathcal{O}\Big(D\Big[M^3 + (2N_B+5)M^2 + (2N_BN_A + 2N_A + 2N_B + 2)M + \Big(2N_B^3 + 2N_B^2 + 2N_BN_A\Big)\Big]\Big) \quad (40)$$

float-point operations (FLOPs), where D denotes the maximum number of alternating iteration.

IV. PROPOSED LOW-COMPLEXITY MAX-RPS-ZF SCHEME

In this section, a maximizing RPS alternate optimization method is proposed to reduce computational complexity. In accordance with the zero-forcing principle, the receive beamforming vectors $\mathbf{u}_{B1}$ and $\mathbf{u}_{B2}$ satisfy

$$\mathbf{u}_{B1}^H\mathbf{H}_{AB}^H = \mathbf{0}_{1\times N_A},\ \mathbf{u}_{E1}^H\mathbf{H}_{AE}^H = \mathbf{0}_{1\times N_A}, \quad (41)$$

$$\mathbf{u}_{B2}^H\mathbf{H}_{IB}^H = \mathbf{0}_{1\times M},\ \mathbf{u}_{E2}^H\mathbf{H}_{IE}^H = \mathbf{0}_{1\times M}, \quad (42)$$

which means that the RBF vector $\mathbf{u}_{B1}$ is only used to receive the CM reflected from the IRS, and $\mathbf{u}_{B2}$ is used to receive the CM through the direct path. The received signals at Bob and Eve are

$$y_{B1} = \mathbf{u}_{B1}^H\Big[\sqrt{\beta_1 P_s g_{AIB}}\mathbf{H}_{IB}^H\boldsymbol{\Theta}\mathbf{H}_{AI}\mathbf{v}_1x_1 + \sqrt{\beta_2 P_s g_{AIB}}\mathbf{H}_{IB}^H\boldsymbol{\Theta}\mathbf{H}_{AI}\mathbf{v}_2x_2 + \mathbf{n}_B\Big], \quad (43)$$

$$y_{B2} = \mathbf{u}_{B2}^H\Big[\sqrt{\beta_1 P_s g_{AB}}\mathbf{H}_{AB}^H\mathbf{v}_1x_1 + \sqrt{\beta_2 P_s g_{AB}}\mathbf{H}_{AB}^H\mathbf{v}_2x_2 + \mathbf{n}_B\Big], \quad (44)$$

and

$$y_{E1} = \mathbf{u}_{E1}^H\Big[\sqrt{\beta_1 P_s g_{AIE}}\mathbf{H}_{IE}^H\boldsymbol{\Theta}\mathbf{H}_{AI}\mathbf{v}_1x_1 + \sqrt{\beta_2 P_s g_{AIE}}\mathbf{H}_{IE}^H\boldsymbol{\Theta}\mathbf{H}_{AI}\mathbf{v}_2x_2 + \mathbf{n}_E\Big], \quad (45)$$

$$y_{E2} = \mathbf{u}_{E2}^H\Big[\sqrt{\beta_1 P_s g_{AE}}\mathbf{H}_{AE}^H\mathbf{v}_1x_1 + \sqrt{\beta_2 P_s g_{AE}}\mathbf{H}_{AE}^H\mathbf{v}_2x_2 + \sqrt{\beta_3 P_s g_{AE}}\mathbf{H}_{AE}^H\mathbf{P}_{AN}\mathbf{z} + \mathbf{n}_E\Big], \quad (46)$$

respectively.

Then, the optimization problem of Max-RPS in (21) can be casted as follows

$$\max_{\mathbf{u}_{B1},\mathbf{u}_{B2},\boldsymbol{\Theta}} \ \beta_1 P_s\mathbf{u}_{B1}^H\mathbf{H}_B\mathbf{v}_1\mathbf{v}_1^H\mathbf{H}_B^H\mathbf{u}_{B1} + \beta_2 P_s\mathbf{u}_{B2}^H\mathbf{H}_B\mathbf{v}_2\mathbf{v}_2^H\mathbf{H}_B^H\mathbf{u}_{B2} \quad (47a)$$

$$\text{s.t.}\ \ \mathbf{u}_{B1}^H\mathbf{H}_{AB}^H = \mathbf{0}_{1\times N_A},\ \ \mathbf{u}_{B2}^H\mathbf{H}_{IB}^H = \mathbf{0}_{1\times M}, \quad (47b)$$

$$\mathbf{u}_{B1}^H\mathbf{u}_{B1} = 1,\ \ \mathbf{u}_{B2}^H\mathbf{u}_{B2} = 1, \quad (47c)$$

$$|\Theta_i| = 1,\ \ i = 1,\ldots,M. \quad (47d)$$

In what follows, we consider to optimal RBF vectors and IRS PSM by alternately calculating $\mathbf{u}_{B1}$, $\mathbf{u}_{B2}$, and $\boldsymbol{\Theta}$.

A. OPTIMIZE RBF VECTORS U_{B1} AND U_{B2} GIVEN IRS PSM Θ

In this section, we regard $\boldsymbol{\Theta}$ as a given constant matrix, and the optimization problem of Max-RPS at Bob related to RBF $\mathbf{u}_{B1}$ can be simplified to

$$\max_{\mathbf{u}_{B1}} \ \beta_1 P_s g_{AIB}\mathbf{u}_{B1}^H\mathbf{H}_{IB}^H\boldsymbol{\Theta}\mathbf{H}_{AI}\mathbf{v}_1\mathbf{v}_1^H\mathbf{H}_{AI}^H\boldsymbol{\Theta}^H\mathbf{H}_{IB}\mathbf{u}_{B1} \quad (48a)$$

$$\text{s.t.}\ \ \mathbf{u}_{B1}^H\mathbf{u}_{B1} = 1. \quad (48b)$$

Based on the Rayleigh-Ritz theorem, the optimal RBF vector $\mathbf{u}_{B1}$ can be derived from the eigenvector corresponding to the largest eigenvalue of the matrix $\beta_1 P_s g_{AIB}\mathbf{H}_{IB}^H\boldsymbol{\Theta}\mathbf{H}_{AI}\mathbf{v}_1\mathbf{v}_1^H\mathbf{H}_{AI}^H\boldsymbol{\Theta}^H\mathbf{H}_{IB}$.

Similarly, given the determined or known $\mathbf{u}_{B1}$ and $\boldsymbol{\Theta}$, the subproblem to optimize $\mathbf{u}_{B2}$ can be expressed as follows

$$\max_{\mathbf{u}_{B2}} \ \beta_2 P_s g_{AB}\mathbf{u}_{B2}^H\mathbf{H}_{AB}^H\mathbf{v}_2\mathbf{v}_2^H\mathbf{H}_{AB}\mathbf{u}_{B2} \quad (49a)$$

$$\text{s.t.}\ \ \mathbf{u}_{B2}^H\mathbf{u}_{B2} = 1. \quad (49b)$$

In accordance with the Rayleigh-Ritz theorem, the optimal $\mathbf{u}_{B2}$ can be obtained from the eigenvector corresponding to the largest eigenvalue of the matrix $\beta_2 P_s g_{AB}\mathbf{H}_{AB}^H\mathbf{v}_2\mathbf{v}_2^H\mathbf{H}_{AB}$.

B. OPTIMIZE IRS PSM Θ GIVEN THE RBF VECTORS U_{B1} AND U_{B2}

Since the second item of the objective function in (47) are independent of $\boldsymbol{\theta}$, the subproblem to optimize $\boldsymbol{\theta}$ can be expressed as follows

$$\max_{\boldsymbol{\theta}} \ \boldsymbol{\theta}^H\mathbf{w}_{h_{AIB1}}\mathbf{w}_{h_{AIB1}}^H\boldsymbol{\theta} \quad (50a)$$

$$\text{s.t.}\ \ (29). \quad (50b)$$

According to the Rayleigh-Ritz theorem, the optimal $\boldsymbol{\theta}$ can be derived from the eigenvector corresponding to the largest eigenvalue of the matrix $\mathbf{w}_{h_{AIB1}}\mathbf{w}_{h_{AIB1}}^H$.

C. OVERALL ALGORITHM

First, we can obtain a new objective function according to the zero-forcing criterion. Then, fix IRS PSM $\boldsymbol{\Theta}$ and use the Rayleigh-Ritz theorem to obtain the RBF vectors $\mathbf{u}_{B1}$, $\mathbf{u}_{B2}$. Next, fix the $\mathbf{u}_{B1}$ and $\mathbf{u}_{B2}$, convert the objective variable $\boldsymbol{\Theta}$ into the phase shift vector $\boldsymbol{\theta}$, and obtain the optimal $\boldsymbol{\theta}$ by the Rayleigh-Ritz theorem. Since the IRS phase-shift restriction of (29), we reform $\boldsymbol{\theta} = \exp\{j\angle(\boldsymbol{\theta})\}$, $\boldsymbol{\Theta} = \text{diag}\{\boldsymbol{\theta}\}$. Finally, loop the above steps, and solve $\mathbf{u}_{B1}$, $\mathbf{u}_{B2}$ and $\boldsymbol{\Theta}$ alternately until the termination condition is satisfied.

The computational complexity of the proposed Max-RPS-ZF algorithm is

$$\mathcal{O}\Big(L\Big[M^3 + (2N_B+1)M^2 + \Big(2N_B^3 + 2N_B^2\Big)\Big]\Big) \quad (51)$$

FLOPs, where L denotes the maximum number of alternating iteration.

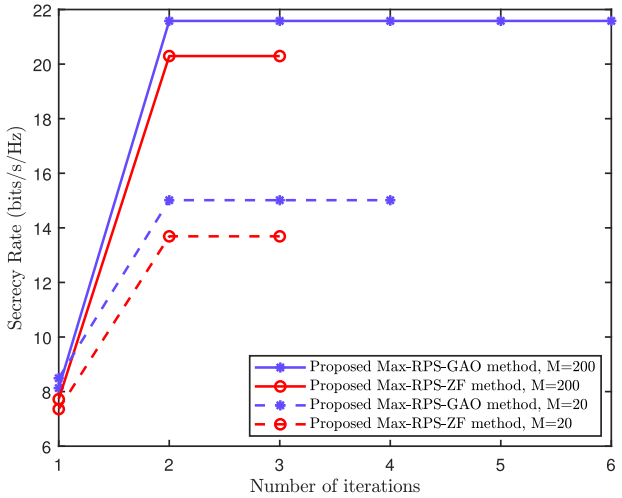

FIGURE 2. Convergence of proposed algorithms at different number of IRS phase-shift elements.

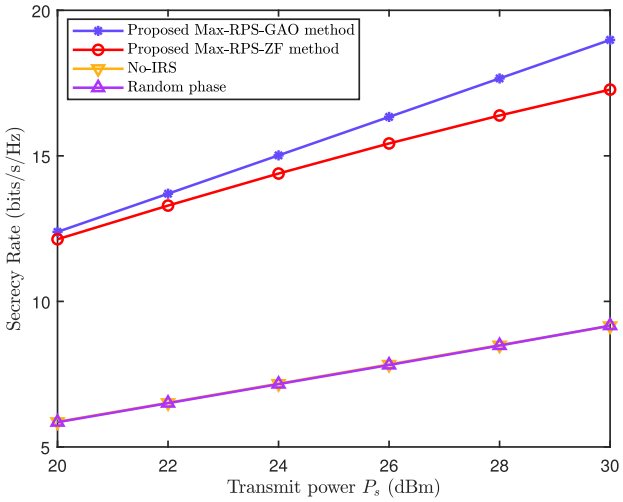

FIGURE 3. Secrecy rate versus the transmit power P_S.

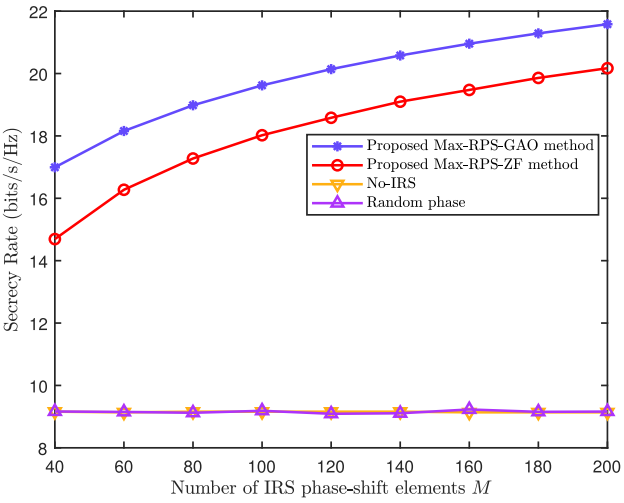

FIGURE 4. Secrecy rate versus the number of IRS phase-shift elements M.

V. SIMULATION RESULTS

In this section, simulations are presented to evaluate the performance of the proposed two schemes. The system default parameters are set as follows: $P_s = 30$ dBm, $\beta_1 = \beta_2 = 0.4$, $\beta_3 = 0.2$, $N_A = 16$, $N_B = N_E = 4$, $M = 80$. The distances of Alice-to-IRS, Alice-to-Bob, and Alice-to-Eve are set as $d_{AI} = 10$ m, $d_{AB} = 50$ m, and $d_{AE} = 50$ m, respectively. The angles of departure (AoDs) of each channel are set as $\theta^t_{AI} = 5\pi/36$, $\theta^t_{AB} = 11\pi/36$, and $\theta^t_{AE} = \pi/3$, respectively. Since the AoD and distance of each channel are given, the channel state information (CSI) of each channel in IRS-aided DM system can be determined.

In what follows, there are two benchmark schemes used to compare with our proposed methods:

1) *Random phase:* The phase for each reflection element of IRS is uniformly and independently generated from $[0, 2\pi)$.
2) *No-IRS:* We assume that the IRS related channel matrices are zero matrices, i.e., $\mathbf{H}_{AI} = \mathbf{0}$, $\mathbf{H}_{IB} = \mathbf{0}$, and $\mathbf{H}_{IE} = \mathbf{0}$.

Fig. 2 plots the curves of SR versus number of iterations for different number of phase shifters $M = 20, 200$. It is observed from Fig. 2 that as the number of iterations increases, the SR performances of the proposed Max-RPS-GAO and Max-RPS-ZF algorithms increase gradually and finally converge to a SR floor. In addition, compared with the proposed Max-RPS-GAO algorithm, the convergence rate of proposed Max-RPS-ZF algorithm is faster. From the perspective of computational complexity, when $M = 200$, the maximum number of alternating iterations of the proposed Max-RPS-GAO and Max-RPS-ZF algorithms are $D = 6$ and $L = 3$, respectively. According to (40) and (51), when the number of M tends to large scale, the computational complexity of the proposed Max-RPS-ZF algorithm is lower than that of the proposed Max-RPS-GAO algorithm.

Fig. 3 demonstrates the curves of SR versus transmit power P_s of the two proposed methods and two benchmark schemes. It can be seen from this figure that the SR of four schemes increases gradually with increases of the transmit power, and the SR performances of the proposed Max-RPS-GAO and Max-RPS-ZF methods are approximately double that of the no-IRS and random phase schemes regardless of the transmit power. Moreover, the difference of the SR between the no-IRS scheme and random phase scheme is negligible. This implies that optimizing the IRS phase shift can bring a significant performance improvement.

Fig. 4 illustrates the curves of SR versus the number of IRS phase shifters elements M of two proposed methods and two benchmark schemes. Compared to the no-IRS and no-PSM optimization schemes, the proposed Max-RPS-GAO and Max-RPS-ZF algorithms can significantly improve the SR performance of the DM system as the number of IRS phase-shift elements M increases. Even with a value of

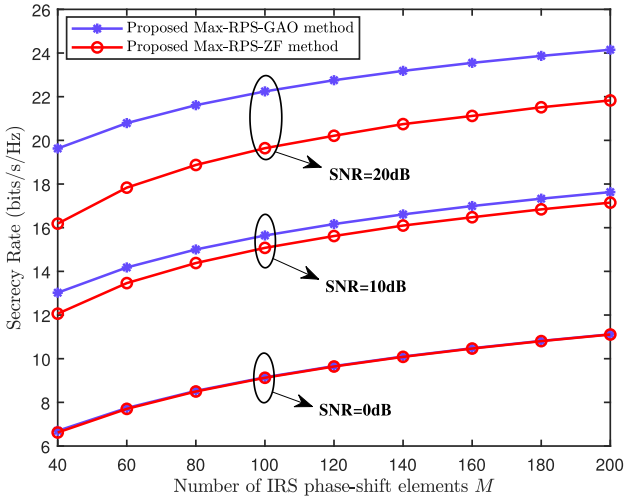

FIGURE 5. Secrecy rate versus the number of IRS phase-shift elements M in three different SNRs.

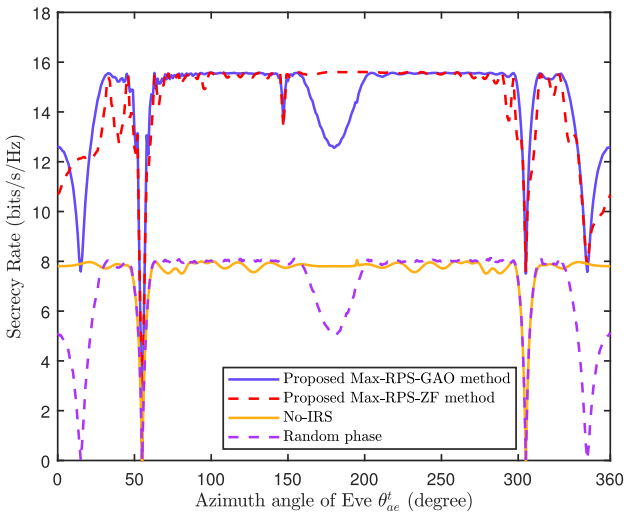

FIGURE 6. Secrecy rate versus the azimuth angle of Eve θ_{AE}^t.

M as $M = 40$, the SRs of the Max-RPS-GAO and Max-RPS-ZF methods are increased by about 86% and 61%, respectively. Furthermore, it can reflect the superiority of designing and optimizing the PSM of IRS, and the importance of constructing IRS-assisted multipath transmission system.

Fig. 5 shows the SR versus the number of IRS phase shifters elements M ranging from 40 to 200 in three different SNR scenarios: (1) SNR = 0dB, (2) SNR = 10dB, and (3) SNR = 20dB. It can be seen from the figure that in low SNR region, the difference in SR performance achieved between the Max-RPS-GAO and Max-RPS-ZF algorithms is trivial. However, the difference in SR performance between the two proposed algorithms gradually increases as the SNR increases, and the difference of SR is about 2 bits/s/Hz when the SNR is equal to 20dB.

Fig. 6 shows the SR versus the azimuth angle θ_{AE}^t of Eve, where θ_{AE}^t changes from 0 to 2π, $\theta_{AI}^t = \pi/12$, and $d_{AB} = d_{AE} = 100$m. Since the transmitter and receiver are both linear arrays, the SR performance of $\theta_{AE}^t \in (\pi, 2\pi)$ and $\theta_{AE}^t \in (0, \pi)$ are almost symmetrical to each other. Observing Fig. 6, once Eve and Bob have the same direction angle, i.e., $\theta_{AE}^t = \theta_{AB}^t = 11\pi/36$, the SR performance of the four schemes will all decline sharply. This is because Eve is located on the direct path from the Alice to Bob, enabling Eve to eavesdrop on CMs to the greatest extent. Nevertheless, when $\theta_{AE}^t = \theta_{AB}^t$, the proposed Max-RPS-GAO method still obtains the best SR performance.

VI. CONCLUSION

In this paper, we have proposed two alternating iteration optimization schemes, called Max-RPS-GAO algorithm and Max-RPS-ZF algorithm, designing the RBF vectors and PSM in an IRS-aided DM network. The former obtains two RBF vectors and the PSM of IRS by employing the Rayleigh-Ritz theorem and derivative operation, and the latter uses the zero-forcing criterion to separate two RBF vectors and IRS PSM, such that the two-path CMs from the direct path and the IRS reflected path are independently recovered. Simulation results showed that, compared with the no-IRS-assisted scheme and no-PSM optimization scheme, the proposed Max-RPS-GAO and Max-RPS-ZF methods can significantly improve the SR performance of the DM system as the number of IRS phase shift elements tends to large scale. Compared to the Max-RPS-GAO, a faster convergence speed and a lower computational complexity can be achieved by the proposed Max-RPS-ZF method. The proposed methods may be applied to the future wireless networks like unmanned aerial vehicle network, satellite communications, vehicle-to-everything, even sixth generation.

REFERENCES

[1] A. Mukherjee, S. A. A. Fakoorian, J. Huang, and A. L. Swindlehurst, "Principles of physical layer security in multiuser wireless networks: A survey," *IEEE Commun. Surveys Tuts*, vol. 16, no. 3, pp. 1550–1573, 3rd Quart., 2014.

[2] N. Yang, S. Yan, J. Yuan, R. Malaney, R. Subramanian, and I. Land, "Artificial noise: Transmission optimization in multi-input single-output wiretap channels," *IEEE Trans. Commun.*, vol. 63, no. 5, pp. 1771–1783, May 2015.

[3] S. V. Pecchetti and R. Bose, "Channel-aware artificial intersymbol interference for enhancing physical layer security," *IEEE Commun. Lett.*, vol. 23, no. 7, pp. 1182–1185, Jul. 2019.

[4] H. M. Wang, Q. Yin, and X.-G. Xia, "Distributed beamforming for physical-layer security of two-way relay networks," *IEEE Trans. Signal Process.*, vol. 60, no. 7, pp. 3532–3545, Jul. 2012.

[5] N. Zhao, F. R. Yu, M. Li, and V. C. M. Leung, "Anti-eavesdropping schemes for interference alignment (IA)-based wireless networks," *IEEE Trans. Wireless Commun.*, vol. 15, no. 8, pp. 5719–5732, Aug. 2016.

[6] N. Yang, P. L. Yeoh, M. Elkashlan, R. Schober, and J. Yuan, "MIMO wiretap channels: A secure transmission using transmit antenna selection and receive generalized selection combining," *IEEE Commun. Lett.*, vol. 17, no. 9, pp. 1754–1757, Sep. 2013.

[7] Y. Zou, J. Zhu, X. Li, and L. Hanzo, "Relay selection for wireless communications against eavesdropping: A security-reliability trade-off perspective," *IEEE Netw.*, vol. 30, no. 5, pp. 74–79, Sep./Oct. 2016.

[8] J. M. Hamamreh, H. M. Furqan, and H. Arslan, "Classifications and applications of physical layer security techniques for confidentiality: A comprehensive survey," *IEEE Commun. Surveys Tuts.*, vol. 21, no. 2, pp. 1773–1828, 2nd Quart., 2019.

[9] L. Wang, Z. Zhang, M. Dong, L. Wang, Z. Cao, and Y. Yang, "Securing named data networking: Attribute-based encryption and beyond," *IEEE Commun. Mag*, vol. 56, no. 11, pp. 76–81, Nov. 2018.
[10] Y. Wu, R. Schober, D. W. K. Ng, C. Xiao, and G. Caire, "Secure massive MIMO transmission with an active eavesdropper," *IEEE Trans. Inf. Theory*, vol. 62, no. 7, pp. 3880–3900, Jul. 2016.
[11] Y.-W. P. Hong, P.-C. Lan, and C.-C. J. Kuo, "Enhancing physical-layer secrecy in multiantenna wireless systems: An overview of signal processing approaches," *IEEE Commun. Mag.*, vol. 30, no. 5, pp. 29–40, Sep. 2013.
[12] W. Yang, X. Lu, S. Yan, F. Shu, and Z. Li, "Age of information for short-packet covert communication," *IEEE Wireless Commun. Lett.*, vol. 10, no. 9, pp. 1890–1894, Sep. 2021.
[13] Q. Cheng, S. Wang, V. Fusco, F. Wnag, J. Zhu, and C. Gu, "Physical-layer security for frequency diverse array-based directional modulation in fluctuating two-ray fading channels," *IEEE Trans. Wireless Commun.*, vol. 20, no. 7, pp. 4190–4204, Jul. 2021.
[14] W.-Q. Wang and Z. Zheng, "Hybrid MIMO and phased-array directional modulation for physical layer security in mmWave wireless communications," *IEEE J. Sel. Areas Commun*, vol. 36, no. 7, pp. 1383–1396, Jul. 2018.
[15] S. Y. Nusenu, "Development of frequency modulated array antennas for millimeter-wave communications," *Wireless Commun. Mobile Comput.*, pp. 1–16, Apr. 2019.
[16] M. P. Daly, E. L. Daly, and J. T. Bernhard, "Demonstration of directional modulation using a phased array," *IEEE Trans. Antennas Propag.*, vol. 58, no. 5, pp. 1545–1550, May 2010.
[17] F. Shu, X. Wu, J. Hu, J. Li, R. Chen, and J. Wang, "Secure and precise wireless transmission for random-subcarrier-selection-based directional modulation transmit antenna array," *IEEE J. Sel. Areas Commun.*, vol. 36, no. 4, pp. 890–904, Apr. 2018.
[18] B. Qiu, L. Wang, X. Yang, and J. Xie, "Security enhancement of directional modulation scheme against hybrid eavesdroppers," in *Proc. Gen. Assem. Sci. Symp. Int. Union Radio Sci. (URSI GASS)*, Sep. 2022, pp. 1–4.
[19] M. P. Daly and J. T. Bernhard, "Directional modulation technique for phased arrays," *IEEE Trans. Antennas Propag.*, vol. 57, no. 9, pp. 2633–2640, Sep. 2009.
[20] F. Shu, X. Wu, J. Li, R. Chen, and B. Vucetic, "Robust synthesis scheme for secure multi-beam directional modulation in broadcasting systems," *IEEE Access*, vol. 4, pp. 6614–6623, 2016.
[21] B. Zhang and W. Liu, "Multi-carrier based phased antenna array design for directional modulation," *IET Microw. Antennas Propag.*, vol. 12, no. 5, pp. 765–772, 2018.
[22] H. Zhang, Y. Xiao, Y. Xiao, and W. Xiang, "Impact of imperfect angle estimation on spatial and directional modulation," *IEEE Access*, vol. 8, pp. 7081–7092, 2020.
[23] Y. Teng *et al.*, "Low-complexity and high-performance receive beamforming for secure directional modulaion networks against an eavesdropping-enabled full-duplex attacker," *Sci. China Inf. Sci.*, vol. 65, Jan. 2022, Art. no. 119302.
[24] R. Dong, B. Shi, X. Zhan, F. Shu, and J. Wang, "Performance analysis of massive hybrid directional modulation with mixed phase shifters," *IEEE Trans. Veh. Technol.*, vol. 71, no. 5, pp. 5604–5608, May 2022.
[25] C. Li, H. J. Yang, F. Sun, J. M. Cioffi, and L. Yang, "Multiuser overhearing for cooperative two-way multiantenna relays," *IEEE Trans. Veh. Technol.*, vol. 65, no. 5, pp. 3796–3802, May 2016.
[26] C. Li, F. Sun, J. M. Cioffi, and L. Yang, "Energy efficient MIMO relay transmissions via joint power allocations," *IEEE Trans. Circuits Syst. II, Exp. Briefs*, vol. 61, no. 7, pp. 531–535, Jul. 2014.
[27] C. Li, X. Wang, L. Yang, and W.-P. Zhu, "A joint source and relay power allocation scheme for a class of MIMO relay systems," *IEEE Trans. Signal Process.*, vol. 57, no. 12, pp. 4852–4860, Dec. 2009.
[28] Q. Wu and R. Zhang, "Towards smart and reconfigurable environment: Intelligent reflecting surface aided wireless network," *IEEE Commun. Mag.*, vol. 58, no. 1, pp. 106–112, Jan. 2020.
[29] F. Shu *et al.*, "Beamforming and transmit power design for intelligent reconfigurable surface-aided secure spatial modulation," *IEEE J. Sel. Areas Commun.*, early access, May 5, 2022, doi: 10.1109/JSTSP.2022.3172682.
[30] C. Huang, A. Zappone, G. C. Alexandropoulos, M. Debbah, and C. Yuen, "Reconfigurable intelligent surfaces for energy efficiency in wireless communication," *IEEE Trans. Wireless Commun.*, vol. 18, no. 8, pp. 5218–5233, Aug. 2019.
[31] X. Pang, M. Sheng, N. Zhao, J. Tang, D. Niyato, and K.-K. Wong, "When UAV meets IRS: Expanding air-ground networks via passive reflection," *IEEE Wireless Commun*, vol. 28, no. 5, pp. 164–170, Oct. 2021.
[32] M. Di Renzo *et al.*, "Smart radio environments empowered by reconfigurable intelligent surfaces: How it works, state of research, and the road ahead," *IEEE J. Sel. Areas Commun.*, vol. 38, no. 11, pp. 2450–2525, Nov. 2020.
[33] W. Tang *et al.*, "MIMO transmission through reconfigurable intelligent surface: System design, analysis, and implementation," *IEEE J. Sel. Areas Commun.*, vol. 38, no. 11, pp. 2683–2699, Nov. 2020.
[34] R. Dong *et al.*, "Performance analysis of wireless network aided by discrete-phase-shifter IRS," *J. Commun. Netw.*, to be published.
[35] Q. Wu and R. Zhang, "Beamforming optimization for wireless network aided by intelligent reflecting surface with discrete phase shifts," *IEEE Trans. Commun.*, vol. 68, no. 3, pp. 1838–1851, Mar. 2020.
[36] M. Cui, G. Zhang, and R. Zhang, "Secure wireless communication via intelligent reflecting surface," *IEEE Wireless Commun. Lett.*, vol. 8, no. 5, pp. 1410–1414, Oct. 2019.
[37] X. Lu, W. Yang, X. Guan, Q. Wu, and Y. Cai, "Robust and secure beamforming for intelligent reflecting surface aided mmWave MISO systems," *IEEE Wireless Commun. Lett.*, vol. 9, no. 12, pp. 2068–2071, Dec. 2020.
[38] X. Pang, N. Zhao, J. Tang, C. Wu, D. Niyato, and K.-K. Wong, "IRS-assisted secure UAV transmission via joint trajectory and beamforming design," *IEEE Trans. Commun.*, vol. 70, no. 2, pp. 1140–1152, Feb. 2022.
[39] Q. Wu and R. Zhang, "Intelligent reflecting surface enhanced wireless network via joint active and passive beamforming," *IEEE Trans. Wireless Commun.*, vol. 18, no. 11, pp. 5394–5409, Nov. 2019.
[40] C. Pan *et al.*, "Multicell MIMO communications relaying on intelligent reflecting surfaces," *IEEE Trans. Wireless Commun.*, vol. 19, no. 8, pp. 5218–5233, Aug. 2020.
[41] X. Wang *et al.*, "Beamforming design for IRS-aided decode-and-forward relay wireless network," *IEEE Trans. Green Commun. Netw.*, vol. 6, no. 1, pp. 198–207, Mar. 2022.
[42] J.-B. Wang, X. Wang, F. Yang, H. Zhang, M. Lin, and J. Wang, "Intelligent reflecting surface aided millimeter wave communication using subarray-connected structure," *IEEE Trans. Veh. Techol.*, vol. 71, no. 5, pp. 5581–5586, May 2022.
[43] L. Lai, J. Hu, Y. Chen, H. Zheng, and N. Yang, "Directional modulation-enabled secure transmission with intelligent reflecting surface," in *Proc. 3rd IEEE Int. Conf. Inf. Commun. Signal Process. (ICICSP)*, Sep. 2020, pp. 450–453.
[44] R. Dong, F. Shu, R. Chen, Y. Wu, C. Pan, and J. Wang. "Beamforming and power allocation for double-RIS-aided two-way directional modulation network." [Online]. Available: https://arxiv.org/abs/2201.09063 (Accessed: Jan. 2022).
[45] F. Shu *et al.*, "Enhanced secrecy rate maximization for directional modulation networks via IRS," *IEEE Trans. Commun.*, vol. 69, no. 12, pp. 8388–8401, Dec. 2021.
[46] G. Golub and C. Van Loan, *Matrix Computations*, 3rd Quart. Baltimore, MD, USA: Johns Hopkins Univ. Press, 1996.

RONGEN DONG is currently pursuing the Ph.D. degree with the School of Information and Communication Engineer, Hainan University, China. Her research interests include physical layer security and directional modulation networks.

SHAOHUA JIANG was born in Shandong, china, in 1971. She received the Master of Science degree in agricultural extension from Shandong Agricultural University in 2005. She is currently an Associate Professor with the School of Electrical and Mechanical Engineering, Weifang Vocational College. Her research interests include theory and practice of mechanical design.

XINHAI HUA was born in Anhui, china, in 1974. He received the Ph.D. degree from Nanjing University in 2015. He is currently the Vice President with ZTE Corporation, the General Manager of the Multimedia Video Product Department. His main research directions are wireless network, cloud computing, IP-based video product technology and solutions, and security solutions of video service, technology and product solutions of content distribution.

YIN TENG received the B.S. degree from the ZiJin College, Nanjing University of Science and Technology, Nanjing, China, in 2019, and the M.S. degree from the Nanjing University of Science and Technology in 2022. Her research interests include wireless communication, physical layer security, and directional modulation networks.

FENG SHU (Member, IEEE) was born in 1973. He received the B.S. degree from Fuyang Teaching College, Fuyang, China, in 1994, the M.S. degree from Xidian University, Xian, China, in 1997, and the Ph.D. degree from Southeast University, Nanjing, China, in 2002. From July 2007 to September 2007, he was a Visiting Scholar with the Royal Melbourne Institute of Technology (RMIT University), Australia. From September 2009 to September 2010, he was a Visiting Postdoctoral Fellow with the University of Texas, Dallas, Richardson, TX, USA. From October 2005 to November 2020, he was with the School of Electronic and Optical Engineering, Nanjing University of Science and Technology, Nanjing, where he was promoted from Associate Professor to a Full Professor of Supervising Ph.D. students in 2013. Since December 2020, he has been with the School of Information and Communication Engineering, Hainan University, Haikou, China, where he is currently a Professor and a Supervisor of Ph.D. and graduate students. He has authored or coauthored more than 300 in archival journals with more than 120 papers on IEEE Journals and 180 SCI-indexed papers. His citations are 4309. He holds 23 Chinese patents and also are PI or CoPI for six national projects. His research interests include wireless networks, wireless location, and array signal processing. He is awarded with the Leading-talent Plan of Hainan, China, in 2020, Fujian hundred-talent plan of Fujian Province in 2018, and the Mingjian Scholar Chair Professor in 2015. He was an IEEE TRANSACTIONS ON COMMUNICATIONS Exemplary Reviewer for 2020. He is currently the Editor for IEEE WIRELESS COMMUNICATIONS LETTERS. He had ever been the Editor for IEEE SYSTEMS JOURNAL from 2019 to 2021 and IEEE ACCESS from 2016 to 2018.

JIANGZHOU WANG (Fellow, IEEE) has been a Professor with the University of Kent, U.K since 2005. He was an IEEE Distinguished Lecturer from 2013 to 2014. He has published over 400 papers and four books in the areas of wireless communications. He was a recipient of the Best Paper Award from the IEEE GLOBECOM2012. He has served as an Editor for a number of international journals, including IEEE TRANSACTIONS ON COMMUNICATIONS from 1998 to 2013. He was the Technical Program Chair of the 2019 IEEE International Conference on Communications (ICC2019), Shanghai, the Executive Chair of the IEEE ICC2015, London, and the Technical Program Chair of the IEEE WCNC2013. He is a Fellow of the Royal Academy of Engineering, U.K., and IET.